Effects of surface forcing on the seasonal cycle of the eastern equatorial Pacific

D.E. Harrison, A.M. Chiodi and G.A. Vecchi

June 2009

Abstract

The roles of zonal and meridional wind stress and of surface heat flux in the seasonal cycle of sea surface temperature (SST) are examined with a primitive equation (PE) model of the tropical Pacific Ocean. While a variety of previous numerical and observational studies have examined the seasonal cycle of SST in the eastern tropical Pacific, it is noteworthy that different mechanisms have been invoked as primary in each case. These studies also reach different conclusions concerning the relative importance of the different components of surface forcing. Here, we perform a series of numerical experiments in which different components of the surface forcing are eliminated and the resulting upper ocean variability is compared with that of the climatological experiment. The model used for these experiments reproduces a realistic climatological seasonal cycle, in which SST emerges as an independent quantity. We find that the different cases all produce qualitatively reasonable seasonal cycles of SST, although only the most complete model is also able to reproduce the seasonal cycle of near surface

currents, tropical instability waves (TIWs), and net surface heat fluxes consistent with historical observations. These results indicate that simply reproducing a qualitatively accurate seasonal cycle of SST does not necessarily allow meaningful conclusions about the processes that control the seasonal cycle of SST to be made. The results described here also suggests that a model simulation must at least reproduce all the documented near surface kinematic features of the equatorial Pacific cold tongue region reasonably well, before accurate inferences can be made from model experiments. This provides useful guidelines to current efforts to develop and evaluate more complex fully coupled air-sea models and shows that results for simple or intermediate ocean models that do not have this level of fidelity to the observations will be difficult to interpret.

1. Introduction

The seasonal cycle and interannual variation of tropical Pacific sea surface temperature (SST) has been the focus of considerable research, as work continues to try to understand and to predict the El Niño-Southern Oscillation (ENSO) phenomenon. The known influence of ENSO on global seasonal climate anomalies makes it, and by association, the seasonal cycle of SST, much scrutinized features of global coupled models that are currently under development and evaluation (e.g. de Szoerke and Xie 2008.)

It has long been known that the eastern equatorial Pacific exhibits a strong annual cycle in SST (range of $\approx$5°C, peak in March) and a much weaker semi-annual cycle (range of $\approx$0.5°C, Levitus 1987). Unlike most ocean regions, however, the relative strengths of these cycles in the equatorial Pacific can not explained by local top-of-the-atmosphere

solar radiation variability, which is dominated by the semi-annual cycle at the equator (downward peaks at the March and September equinoxes.) Thus, the relatively strong annual cycle of SST in the eastern equatorial Pacific must predominantly arise from something other than the local effects of seasonal changes in sun-earth orbital geometry.

Since SST is the primary oceanic variable that affects the atmosphere, there has been much interest in trying to understand its variations. Efforts to model seasonal and interannual SST changes have been made with ocean and coupled air-sea models of different levels of complexity (discussed in detail below.)

The different models encourage upper ocean temperature budgets to be done in different ways and, where direct comparison of results is possible, this seems to produce different SST budgets. In the context of the high resolution PE model, results are particularly sensitive to the depth over which averaging is done to define SST (e.g. a choice of 20 m often yields quite different results from one of 50 m.) Results also appear to be sensitive to the near surface configuration of the ocean model; e.g. in the case of the coupled air-sea model used by Wang and Fu (2001) that explicitly defines the mixed layer depth, it appears that seasonal changes of the model mixed layer depth are important to the seasonal cycle of SST.

Surface heat flux depends on the SST as well as atmospheric variables such as wind speed, air temperature and humidity and cloud cover. Fully coupled air-sea models allow for the simultaneous computation of SST and these atmospheric variables. Considerable success has been made in producing such models, though certain problems,

such as finding a physically realistic parameterization of atmospheric convection and cloud cover persist (Arakawa 2004). Coupled models provide a useful set of consistent surface fluxes and SST, but the upper ocean variability predicted in such models is often significantly influenced by wind stress errors produced from the atmospheric model (e.g. de Szoerke and Xie 2008, DeWitt and Schnieder 1999) Also, the computational costs associated with the fully coupled models often prevent multiple deterministic experiments from being run, as is done here. This study is thus complementary to current efforts to improve the simulation of the seasonal cycle of SST and ENSO in fully couple models, such as those submitted for inclusion in the recent Intergovernmental Panel on Climate Change Fourth Assessment Report (IPCC AR4.)

To examine the mechanisms for the seasonal cycle of SST in the eastern equatorial Pacific, we use an ocean model forced with observed winds and surface heat fluxes that are specified from the model SST and an imposed climatological atmosphere. Since we wish to determine the effects of ocean currents from our model simulations, and ocean currents are driven by winds, using observed wind stress fields is possibly advantageous in this case. On the other hand, care must be taken that the imposed surface heat flux condition does not introduce inconsistencies between oceanic heat advection and surface heat flux, as described by Seager (1995a). To do this, we specify as a "compatibility" condition that any computed parameters that figure into the surface boundary with the atmosphere,that are not imposed directly (e.g., SST, surface heat flux), must be consistent with data[1]. A model that produces realistic currents, a realistic vertical density

[1]In the absence of a complete coupled model, imposition of a more complicated surface heat flux boundary condition to an ocean model (e.g., Kessler et al. 1998; Seager et al. 1988) does not change this. Rather it just creates a more subtle compatibility condition.

structure, and atmospheric parameters that are in "the ballpark" or better may be said to be self-consistent. It is sensible and meaningful to use subsurface velocity and temperature fields from such a model to speculate about oceanic balances and processes. So long as the model's temperature gradient fields agree with observations, it is reasonable to diagnose the role of ocean advection in an PE ocean model that integrates observed wind stress. The subsurface conditions are what is obtained from this exercise, and they are, after all, the things that are the most difficult to measure.

However the near-surface temperature budgets are done, no simple story has evolved to explain how the Pacific warms and cools (either seasonally or interannually), except in the early ocean warming stage of ENSO events (when anomalous zonal advection appears to be a primary warming mechanism, driven either by local or remote reductions in the easterlies). In the seasonal cycle, SST variations appear to result from small imbalances among much larger heat equation terms, particularly nonlinear advection, surface heat flux and vertical mixing. But can we say what combination of circumstances (model and boundary conditions) together make analysis of processes affecting SST meaningful? And if we can reach this state, what can we say about where we are right now in our understanding of these processes?

In this study, the roles of zonal and meridional wind stress, as well as surface heat fluxes, in the upper ocean seasonal cycle are explored with a physically realistic PE model of the Pacific. The climatological seasonal cycle experiment described by Harrison et al. (2000) is the starting point for a series of numerical experiments in which

different components of the surface forcing are eliminated and the resulting upper ocean variability is compared with that of the climatological experiment. The wind fields used are always based on the climatological wind stress field of the tropical Pacific. We examine the relative importance of the surface heat flux, and zonal and meridional wind stress in driving the near-surface seasonal cycle in the extreme eastern Pacific (east of 95°W), in the western Pacific (west of the dateline) and in the predominant trade wind region (95°W–180°W). Previous numerical and observational work is examined in Section 2. Our numerical model is described in Section 3. Because the surface heat flux boundary condition is critical in this context, in Section 3 we discuss the role of our surface heat flux boundary condition in the near-surface heat equation. In Section 4 we compare the results from a series of numerical experiments. Section 5 is a discussion of the main results.

2. Background

Numerical Model Experiments

In an attempt to gain insight into the underlying processes that control SST evolution, in particular the role of meridional wind stress in the seasonal cycle, Philander and Pacanowski (1981) carried out a numerical study using idealized meridional wind stress patterns, with no zonal wind stress and an idealized horizontally uniform density field in a rectangular domain. The numerical model was the same PE model as is used here, but with slightly different parametrization for horizontal diffusion. For their experiments,

the surface heat flux was defined to be proportional to the difference between SST and a reference temperature (25°C). They found that they could produce a modest equatorial cold tongue with a constant stress field. Confining the stress to the eastern part of the basin and adding a periodic component produced some variation in equatorial and near-"coastal" SST while maintaining a cold tongue. They inferred that "SST variations observed in the eastern equatorial Pacific Ocean on seasonal time scales may to a large extent be due to the variability of the local meridional winds", i.e., meridional stress alone may be a substantial factor in both seasonal and interannual SST variation in the equatorial eastern Pacific. A similar model was later used by Philander et al. (1987) to study upper tropical Pacific circulation. In this case, both components of wind stress were applied to the model.

Takeuchi (1988) studied the seasonal variation of the cold water tongue in the eastern tropical Pacific SST, with a Bryan-type 10-level PE model (Bryan 1969; see also Gordon and Corry 1991 for results from a similar model.) A Haney-type surface heat flux parameterization was employed (Haney, 1971), where the heat flux is proportional to the difference between SST and a constant reference temperature (30°C everywhere except near the southern and northern boundaries, where it is set to 12°C in order to supply cold water at the edges of the domain). There was no seasonal variation in thermal forcing; the only seasonal forcing was supplied by the wind stress. Based on his model results, Takeuchi concludes that "the main portion of the cold water tongue is supplied by meridional wind stress-forced upwelling along the eastern boundary several hundred km south of the equator. The upwelled water is advected equatorward along

the coast, the cold water then extends westward along the equator carried by strong westward surface currents. It is a rather surprising conclusion that equatorial upwelling does not contribute to the seasonal variation of SST".

Seager et. al. (1988) studied the tropical Pacific SST climatology with a simple linear 1 1/2-layer model for velocity, but with a nonlinear temperature equation in the upper layer, and with a surface heat flux parameterization that does not include air temperature and humidity. As with several of the other model studies mentioned here, the sensible heat flux is proportional to the difference between SST and a reference temperature. The latent heat flux is parameterized with the surface wind and SST, and solar heating is a function of cloud cover, latitude and (constant) surface albedo. The major elements of the seasonal development of the SST field are seen in the model results. They find that the cold tongue is primarily due not to coastal upwelling or advection of cold water from the south, but to a maximum of cloud cover which induces a minimum of surface heating. They state that: "during northern hemisphere fall, when the SST is a minimum, there is a strong cooling due to (equatorial) upwelling, which overpowers the surface heating. The model indicates that zonal and meridional advection aid the cooling but have significant effects only when the tongue is most developed".

Harrison (1989a) performed a series of numerical hindcasts of the 1982-83 ENSO, for the purpose of exploring which aspects of the tropical surface wind stress field are important in determining SST within the waveguide during 1982-1983. The numerical model used in the Harrison study was the same PE model that is described in the present work,

but the model parameterized the surface heat flux in terms of only the wind speed and the SST; the surface heat flux parametrization assumed constant radiation, but allowed sensible and latent heat flux variations. They found that "meridional wind stress plays a nontrivial, but not dominant role, in the 1982-83 model behavior". Meridional stress could be neglected with very little impact on the upper ocean equatorial temperatures or zonal currents; zonal wind stress appeared to control the evolution of the near-surface ocean hindcast. See also Seager et al. (1989), Latif (1987) and Harrison et al. (1990) for 1982–83 hindcast SST studies using differently configured primitive-equation (PE) ocean models.

Motivated by reports from Seager and Blumenthal (1994) that, in the Cane-type model (Cane 1979) described by them, "inadequate treatment of mixed layer/entrainment processes in upwelling regions of the eastern tropical Pacific leads to a large and seasonally varying error in the model SST", Chen et al. (1994) used an ocean model configured with a variable depth well-mixed upper layer and several deeper isopycnal layers to study the seasonal cycle of SST in the tropical Pacific. In this case, surface fluxes were specified according to the method of Seager et al. (1988). Chen et al. also emphasize the importance of ocean mixing processes, reporting that "It is found that the large SST annual cycle in the eastern equatorial Pacific is, to a large extent, controlled by the annually varying mixed layer depth which, in turn, is mainly determined by the competing effects of solar radiation and wind forcing." The effects of upper ocean model configuration were also discussed by Chang (1994a.)

Köberle and Philander (1994, KP94 hereafter) studied the processes that control seasonal SST variation in the tropical Pacific (20S to 20N) with a PE model similar to the one used here. Seasonally varying wind stress and surface heat flux was applied to the model based on climatological atmospheric conditions and model SST. It was found that this model generally reproduced realistic seasonal SST variations when all surface forcing components were applied. Experiments, similar to some described in the present study, were then performed in which the seasonal variations were alternately removed from surface heat flux and wind stress fields, prior to model integration. Effects of these perturbations varied with location, but analysis of the upper ocean (0-50m depth) heat budget in the eastern equatorial Pacific (defined here as 4°S to $4^{c}irc$N and 104°W to 86°S,) led authors to conclude that, essentially, "...the seasonal cycle variations in heat flux are balanced by seasonal variations in the upwelling of a steady stratification plus the steady upwelling of a seasonally varying stratification." In this case, the seasonally varying stratification is caused by "heat fluxes that modulate mixing processes in the ocean," as opposed to thermocline depth variations, which are said to play a more important role in causing interannual SST variability. The authors also conclude that, elsewhere in the study region, the upper ocean seasonal cycle is essentially caused by net surface heating. Experiments described in the present study revisit the relationship between effects of surface heat and momentum fluxes, but expand upon the study of KP94 by separately considering the effects of zonal and meridional components of wind stress. This was not done in KP94. Also, unlike KP94, the present study focuses only on the near-equatorial region, where oceanic Kelvin waves are prominent features of ocean adjustment to wind stress variations. The conclusions reached in the present

study (discussed below) are in many respects different from those reached by KP94.

Li and Philander (1996) report results from a simple, coupled ocean-atmosphere model, consisting of a Lindzen-Nigam type atmosphere (Lindzen and Nigam 1987) coupled to a Cane-Zebiak type ocean model (Cane 1979; Zebiak and Cane 1987; see also Chang 1996 for a study using a similar model.) Their model is an anomaly model forced by incoming solar radiation with cloud fraction specified as a simple function of model SST. Annual mean SST and wind fields must be specified to the model prior to integration. Experiments were performed that depended on splitting the solar forcing and time-mean model states in to parts that are symmetric and asymmetric about the equator. Authors conclude that it is the asymmetric state that is mainly responsible for the strong annual cycle of SST in the equatorial Pacific; because of time-mean meridional contrasts in eastern equatorial Pacific SST, "the northward winds at the equator will be intense toward the end of the northern summer, relaxed toward the end of southern summer." In their model, modulation of evaporation by these meridional winds drives an annual cycle of SST at the equator of modest amplitude, that "can be augmented by next taking into account the dynamical response of the ocean to the winds." The authors state that the meridional advection of temperature is "of central importance" to the dynamic response in the eastern equatorial Pacific (e.g. 100°W,) and that "the vertical advection of temperature is important primarily because it magnifies the meridional temperature gradient." It is also found that the seasonal cycle in eastern equatorial SST is also augmented by seasonal changes in cloud cover in this model. Interested readers can also consult Giese and Carton (1994), for a coupled-model perspective. In this case,

it was concluded that the coupled Pacific system has a "timescale that allows the annual cycle to be amplified preferentially."

Kessler et. al. (1998, K98 hereafter) report results from a upper ocean GCM of the tropical Pacific. The model consists of a surface wind-forced sigma-layer tropical PE GCM developed by Gent and Cane (1989), with a surface mixed layer formulation developed by Chen et. al. (1994a,b; see also Kraus and Turner, 1967 and Price et. al., 1986) as its upper layer. Their surface heat flux boundary condition was based on the heat flux formulation of Seager et. al., (1988), which requires only cloud cover and wind speed as input. Solar radiation intensity was modulated by cloud fraction, which was adjusted empirically from the observed values to make the mean model SST agree with Levitus (1982). K98 examined the effects of holding meridional and zonal winds at their annual mean values (for dynamics but not for wind mixing or turbulent surface heat flux,) finding that suppressing meridional variability had little effect on the amplitude of the annual cycle in the equatorial region defined by them as the "eastern equatorial Pacific" (120°W and 90°W) and within a few degrees of the equator, and that suppressing zonal wind variability resulted in relatively larger differences from the full forcing runs, but that "rms SST differences from the standard run were not too much larger than the constant meridional wind case". K98 conclude that, to first order, the three-dimensional ocean advective terms in the cold tongue region tend to cancel each other in the annual cycle and "the variations in SST can be described as simply following the variation of net solar radiation at the sea surface (sun minus clouds)".

Borovikov et al. (2000) studied the surface heat balance in the equatorial Pacific using a reduced-gravity model (Schopf and Loughe 1995) consisting of a well-mixed upper layer, and nearly-isopycnal lower layers. Both climatological and interannual variations were discussed. Surface heat flux was specified using the atmospheric mixed-layer model of Seager (1995b,) forced with observed, seasonally varying winds (from two sources), air temperature, specific humidity, solar forcing and cloud cover. The character of the surface heat budget was found to depend substantially on longitude. Borovikov et al. summarize that "In the western Pacific the annual cycle of SST is primarily in response to net surface heat flux. In the central basin [165W-110W] the magnitude of the zonal advection term is comparable to that of the net surface heat flux. In the eastern basin the role of zonal advection is reduced and the vertical mixing and advection are more important."

Fu and Wang (2001) used a coupled ocean-atmosphere model of intermediate complexity to study the seasonal cycle of SST in the equatorial Pacific. They found that, in the absence of an annual variation in the zonal wind, the annual range of SST averaged over much of the eastern equatorial Pacific (4°N-4°S, 120°-90°W) was only reduced by about 20%. Whereas, when the annual variation of the meridional winds was removed, the amplitude of the annual cycle was reduced by a factor of about 50%. They find that, in this region, meridional wind affects SST mainly by changing evaporation, entrainment, meridional advection, and the mixed layer depth. They also conclude that the "seasonal cycle of the zonal wind component plays a major role in reproducing the westward progression of annual warming."

Table 1 summarizes the numerical model studies of the seasonal cycle of the eastern tropical Pacific ocean described above. The type of model used, the forcing imposed at the surface, and the conclusion about what primarily drives the seasonal cycle of SST are listed for each study. While the seasonal cycle of SST is reproduced quite credibly in every case, the forcing used and the conclusions reached vary widely.

Table 1: Summary of numerical model studies of the seasonal cycle of the eastern tropical Pacific ocean. The type of model used, the forcing imposed at the surface, and the conclusion about what primarily drives the seasonal cycles of SST are listed for each study. While the seasonal cycle of SST is reproduced quite credibly in every case, the forcing and the conclusions reached vary widely.

Authors	**Date**	**Model Used**	**Forcing Used**	**Conclusions Reached**
Philander and Pacanowski	1981	PE(MOM)	idealized meridional wind stress; no zonal wind stress; surface heat flux proportional to difference between SST and reference temperature	meridional stress alone produces SST seasonal cycle, meridional stress alone including cold tongue
Seager et al.	1988	linear $1\frac{1}{2}$-layer model for velocity; nonlinear temperature equation in the upper layer	seasonal wind stress forcing; sensible heat flux proportional to the difference between SST and a reference temperature: latent heat flux parameterized with the surface wind and SST; solar heating a function of cloud cover and latitude	cold tongue is primarily due to variations of cloud cover; equatorial upwelling yields strong cooling, zonal and meridional advection have significant effects only when the tongue is most developed
Takeuchi	1988	Bryan-type 10-level PE model	seasonal wind stress forcing; Haney-type surface heat flux parameterization was employed; heat flux is proportional to the difference between SST and a reference temperature	equatorial upwelling does not contribute to SST seasonal cycle cold water tongue is supplied by meridional wind stress-forced upwelling and advection along the eastern boundary; westward surface currents carry cold water westward along the equator
Harrison	1989a	PE(MOM)	seasonal wind stress forcing; surface heat flux parameterized in terms of only the wind speed and the SST; constant radiation	meridional stress can be neglected with little impact on SST cycle; zonal stress appeared to control the evolution of the near-surface ocean hindcast
Köberle and Philander	1994	PE(MOM)	seasonal wind stress forcing; heat fluxes from bulk formula model SST and observed atmospheric fields	eastern equatorial SST seasonal cycle controlled by local wind-induced upwelling and modulation of upwelling by surface heat fluxes

Continued on Next Page...

Table 1 – Continued

Authors	Date	Model Used	Forcing Used	Conclusions Reached
Chang	1994a	$1\frac{1}{2}$-layer reduced gravity model for velocity; two mixed layer configurations	seasonal wind stress forcing; climatological heat flux forcing with surface relaxation to climatological SST	wind-driven ocean dynamics and surface heat flux forcing are important to the eastern equatorial SST seasonal cycle; response to heat flux forcing is larger for variable mixed layer depth case; westward propagations of equatorial seasonal cycle depends on dynamical response to wind; unclear if meridional or zonal component dominates
Chen et al.	1994	reduced gravity PE model; variable depth mixed layer with hybrid mixing; 8 lower sigma layers	seasonal wind stress forcing; heat flux as in Seager (1988)	annual cycle of SST in eastern equatorial Pacific controlled largely by annually varying mixed layer depth; mixed layer depth controlled by solar forcing and wind mixing
Li and Philander	1996	Cane-Zebiak type ocean coupled to Lindzen-Nigam atmosphere	specified time average conditions ; specified solar forcing ; surface solar forcing depends on SST via cloud parameterization; latent heat flux from model SST, winds and empirically determined-near surface humidity	eastern equatorial SST seasonal cycle driven mainly from effects of meridional winds on asymmetric mean state; effects of meridional ocean advection and meridional wind-induced latent heat flux variability mainly drive annual cycle, with some contribution from cloud effects on solar forcing
Chang	1996	Cane-Zebiak type ocean coupled to Lindzen-Nigam atmosphere	specified time average conditions ; seasonally varying solar forcing assuming constant cloudiness	eastern equatorial SST seasonal cycle influenced by zonal and meridional coupling; strong annual SST signal in near-coastal region mainly from meridional coupling; westward expansion of annual variations due to zonal interactions
Kessler et al.	1998	sigma-layer tropical PE GCM	seasonal wind stress forcing; heat flux computed from only cloud cover and wind speed; solar radiation was modulated by cloud fraction and adjusted empirically	SST seasonal cycle can be described as simply following the variation of net solar radiation at the sea surface
Borovikov et al.	2000	reduced gravity quasi-isopycnal model	seasonal wind stress forcing; heat fluxes from Seager (1995b) methods; specified air temperature, humidity, solar forcing and cloud cover	character of surface heat budget highly dependent on longitude; no simple explanation for seasonal cycle; details of heat budgets depend on wind stress used
Fu and Wang	2001	$2\frac{1}{2}$-layer PE atmospheric model, coupled to an ocean with mixed layer, thermocline and motionless deep layer	fully coupled forcing over the tropical Pacific, except cloud amounts are specified for longwave and shortwave radiation	Seasonal cycle of SST in in the eastern equatorial Pacific is primarily due to the effects of meridional wind on entrainment and latent heat flux

Observational Studies

The annual cycle of SST and winds in the equatorial Pacific was documented by Horel (1982,) who described a longitudinal change in the phase of the annual cycle of SST such

that the warmest waters near the Peru coast appear in March, while further west, the warmest temperature occur progressively later and with diminished amplitude. Horel found that the annual cycle in surface wind is dominated by meridional migrations of the trade wind belts, with seasonal flow directed into the summer hemisphere (relative to the annual mean,) and found that the annual cycle in meridional wind is larger that that of the zonal wind. Mitchell and Wallace (1992), after scrutiny of oceanic and atmospheric data and motivated by the Philander and Pacanowski (1981) results, raised the question of the importance of the meridional stress in tropical Pacific SST evolution. In particular, they speculate that the increase in the northward surface winds in response to the onset of the northern summer monsoon may be instrumental in reestablishing equatorial cold tongues. Tozuka and Yamagata (2003) have also suggested that the meridional wind mechanism described by Mitchell and Wallace (1992) is a key pacemaker of the annual cycle in the tropical Pacific, though based on analysis of several observed surface marine variables, Wang (1994) has argued against the hypothesis that monsoonal winds, driven by land heating, cause the near-coastal seasonal evolution of eastern equatorial SST. Based on their analysis, Nigam and Chao (1996) argued that, while the equatorial annual cycle in SST is largely generated by meridional wind induced coastal upwelling west of 110°W, east of here, the "SST annual cycle is driven largely by the coupling of zonal winds and SSTs through equatorial upwelling and zonal SST gradient."[2]

Wang and McPhaden's (1999) analysis Tropical Atmosphere Ocean Array (TAO)

[2]This led Nigam and Chao (1996) to propose a "westward expansion hypothesis" for the seasonal cycle, with similar dynamics to the "slow SST mode" proposed by Neelin (1991), to explain interannual SST variability (see also Chang and Philander 1994 and Xie 1994 for alternative "westward expansion" hypotheses.

buoy array show that the heating of the mixed layer by surface heat fluxes at 0°,110°W is mainly balanced by cooling due to the effects of cooler water being entrained into the mixed layer. They found that meridional advection associated with instability waves significantly warmed the surface at this location and that zonal and meridional advection, surface heating and vertical heat advection were each significantly contribute to the seasonal cycle of SST in this region, with the largest terms being the vertical advection and surface heating[3]. Swenson and Hanson (1999) similarly reported that heat storage, heat export by entrainment of upwelled water and heat export by meridional advection mainly determined the annual heat budget in the eastern equatorial Pacific, although they also reported that zonal heat transport is important to the annual cycle. Whereas Wang and McPhaden found a warming due to meridional advection, Swenson and Hanson (1999) found that meridional currents tend to cool the equatorial eastern Pacific. This discrepancy appears to be a result of the fact that the TAO buoy data examined by Wang and McPhaden resolves the effect of eddy heat transport associated with tropical instability waves (Wang and McPhaden, 1999). Bonjean (2001) used currents from buoy drift and current meter record to estimate that meridional and zonal advection by surface currents are important to the mean heat balance of the central and eastern equatorial Pacific. Bonjean also concludes that the vertical transport of heat must be included to balance net surface heating in the eastern tropical Pacific.

Estimates of upwelling velocity and mean source temperature of upwelled water are given by Wyrtki (1981) and, more recently, by Johnson et al. who found that, averaged

[3]see also Hayes et al. (1991) for a description of mixed layer heating at 0°,110°W and Enfield (1986) for heat budget estimates over the entire equatorial Pacific

over 3.6°S-5.2°N, 170°E-95°W the upwelling velocity peaked at 1.9 ($\pm$0.9) 10^{-5} m/s at 50 m depth, and that, on average, the difference between surface water and source water was 4°C.

Cronin et al. (2006) examined the role of clouds in various locations in the far eastern equatorial Pacific. Their analysis of meteorological buoy based longwave and shortwave downwelling surface fluxes indicates that, over the cold tongue, cloud forcing is stronger when SST is cool. Clouds reduce incoming shortwave radiation as well as increase downwelling longwave radiation. Cronin et al. found that, over all eastern Pacific regions considered, the shortwave radiation effect is larger than the longwave cloud effect and thus, the net effect of clouds is to increase net downwelling radiation when SST is warm in Boreal spring.

3. The Model

The model used here is basically the Philander and Seigel (1985) version of the Bryan-Semtner-Cox (Bryan 1969; Semtner 1974; Cox 1984) primitive equation model that Philander and Pacanowski have developed over the past decades (Pacanowski, 1996). It is used here with 27 levels in the vertical. The upper grid point is at 5 m, with a uniform 10 m grid in the upper 100 m, and increasingly non-uniform deeper; there are 17 levels above 250 m. The horizontal grid is uniform between 10°N and 10°S, with 0.33 degree resolution in latitude and 1.0 degree resolution in longitude. Poleward of 10 degrees the meridional resolution increases non-uniformly, to 50°N and to 25°S. Constant horizon-

tal eddy viscosity (A_m) and heat diffusion (A_h) coefficients are used, with $A_m = 10^7$ cm^2/s and Ah = 2 x 10^7 cm^2/s. Note that our A_m is a factor of two smaller than that used by Philander and Seigel (1985). Subgrid scale mixing in the vertical is done with the Richardson number-dependent mixing formulation described by Pacanowski and Philander (1981). Convective adjustment by the original Bryan formulation will also contribute to vertical mixing if there is sufficient surface cooling. The model was initialized with no motion and with temperature-salinity specified by climatological fields in January (Levitus, 1982). The baseline model $\mathbf{T}^X\mathbf{T}^Y$ (described below) was forced for 15 years by climatological monthly mean surface wind stresses, developed from the COADS [4] marine data set and the Large and Pond (1981) stability-dependent drag coefficient (Harrison, 1989b) [5] and by the Philander and Seigel (1985) surface heat flux parameterization as modified by Harrison (1991) and used more recently by Harrison et al. (2001a,b) and Harrison and Chiodi (2008.) The reference atmospheric temperature field for use in the surface heat flux calculation is the climatological seasonally varying COADS marine data set used in Philander et al. (1987.)

The Surface Heat Flux Boundary Condition

Coupling an ocean model to an atmospheric model would allow simultaneous computation of SST and closely related atmospheric parameters such as cloud cover, wind speed, air temperature, and humidity. With this approach, the surface heat flux emerges natu-

[4] Comprehensive Ocean-Atmosphere Data Set, compiled from ship records (Woodruff et. al., 1987).

[5] The bulk formula $\tau = \rho_a C_D |u| u$ was used to estimate the surface wind stress vector τ (τ^x,τ^y) in terms of the wind speed **u** (u,v) at a height of 10 m above the sea surface, the air density ρ_a and drag coefficient C_D. C_D depends on u, so that an iterative process is required to obtain τ

rally. Such coupled models are under development (Wittenberg 2006; Cai 2002; Schneider 2002; Perigaud 2000; DeWitt 1999; Delecluse 1998; Robertson 1995), and have achieved some measure of success (de Szoeke and Xie 2008; Guilyardi 2006; Davey et al. 2002; Latif et al. 2001; Mechoso et al., 1995). As we have said in the introduction, in the absence of a coupled model, the best we can hope for is a form of 'self-consistency', or compatibility between observations and model predictions. What we lack is direct knowledge of vertical velocity (w) and vertical mixing very near the surface, so we can not say that the model is right; we can only reconcile it with the observations at hand.

The boundary condition that restores SST to climatology is typically something like:

$$Q = \kappa(SST - T_o) \tag{1}$$

where Q is the heat flux (cal/cm^2/s, defined such that positive Q implies heating of the ocean), T_o is the imposed climatological restoring temperature, and κ is a coupling coefficient. This is the surface heat flux condition that has been criticized by Seager et al. (1995a). The basic criticisms are (a) if SST is restored strongly to the seasonal cycle in T_o, SST is fixed by the boundary condition, independent of the model dynamics. In addition, as SST approaches T_o the heat flux goes to zero, which is unphysical, since then the ocean cannot act to transport heat - which we know it does, (b) condition (1) assumes that the atmosphere has an infinite heat capacity, and (c) values for κ required to match data (e.g., Oberhuber 1988) are too large.

The response to (a) and (c) above may be formulated by examining the actual sur-

face heat flux boundary condition used in our model, i.e.,

$$Q(x, y, z, t) = SW(x, y, z, t) - LW - QS(x, y, t) - QE(x, y, t) \tag{2}$$

where SW is solar shortwave heating (a function of latitude y, longitude x, and depth z), LW is the longwave back radiation (set to a constant value of 115 ly/day), QS is the sensible heat flux and QE is the latent heat flux. The only part of (2) that resembles (1) is the sensible heat flux:

$$QS = \rho_a C_d c_{pa} |v| (SST - T_a) \tag{3}$$

where ρ_a is the surface air density, C_d is a drag coefficient (set to a constant value of 1.4 x 10), c_{pa} is the heat capacity of air (set to a constant value of 0.24 cal/g/K), and $|v|$ is the wind speed. QS, v, and SST are functions of latitude and longitude, and are computed for each time step. The externally imposed air temperature (T_a) is also a function of latitude and longitude, and is updated for each time step. But QS is relatively small compared to the short wave solar radiation and latent heat components:

$$SW = (1.1574x10^{-5}) q_s [r exp(-z/\alpha_1) + (1 - r) exp(-z/\alpha_2)] \tag{4}$$

$$QE = \rho_a C_d L |v| (0.662/P_{atm}) [e_s(SST) - H_r e_s(T_a)] \tag{5}$$

where q_s is the shortwave incident on ocean surface (which varies in space and time), r is the shortwave partition for near infrared-radiation (0.58 penetrates below 1 m),

p_{atm} is atmospheric pressure, and $\alpha_{1,2}$ are e-folding scales for the vertical absorption of the short wave radiation with depth z. The shortwave incident on the ocean surface is parameterized with latitude and cloud cover (which is in turn parameterized with SST according to the methods of Harrison 1991). In addition, r and $\alpha_{1,2}$ vary with geographic region (warm pool, central-eastern Pacific, far-eastern Pacific), in general agreement with observations. In (5) L is the latent heat of vaporization per unit mass (595 cal/g), H_r is the relative humidity (taken to be 0.8), and $e_s(T)$ is the saturation vapor temperature.

The boundary condition (2) contains considerably more physics than implied by (1). The mixed condition is not subject to the constraints about which Seager expresses concern; the relaxation term plays only a minor role. In this context, κ as defined by (1) is irrelevant. Killworth et al. (2000) have examined the errors in surface tracers and fluxes that occur from the application of (1) to a model similar to that used here and found that there is a tell-tale phase shift in the seasonal cycle of about a month that occurs as a result of these errors. We refer readers to our results section where it is clear that no such phase shift is apparent in the model results discussed here. As suggested by Killworth, the use of bulk formula to couple an ocean model to a climatological atmosphere has assuaged the concerns raised by Seager.

The equation governing ocean temperature (T) in the model is:

$$\frac{\partial T}{\partial t} = -u\frac{\partial T}{\partial x} - v\frac{\partial T}{\partial y} - w\frac{\partial T}{\partial z} + \frac{\partial}{\partial z}(\kappa_H \frac{\partial T}{\partial z}) + A_H \frac{\partial T}{\partial x} + A_M \frac{\partial T}{\partial y} \tag{6}$$

where t is time, (u,v,w) are velocity components in (x,y,z) directions, ρ and c_p are water density and heat capacity, and κ_H is a vertical diffusivity coefficient. The statement that the SST is fixed by a restoring surface heat flux boundary condition presupposes that near-surface vertical and horizontal advection and diffusion of heat is unimportant. Contrary to this, preliminary examination of this term balance has shown that oceanic advection is of fundamental importance to the annual mean upper ocean heat budget. This can be verified for our baseline experiment (described below) in the included appendix.

The point (b) above is resolved by comparing the heat fluxes computed by the model with observed climatological values (e.g. Esbensen and Kushnir 1981, Oberhuber 1988.) These observed values presumably do not require an infinite atmospheric heat capacity. For surface heat flux, values derived from observations typically have ± 30 W/m^2 errors in Q; we have that level of freedom to work with. As we will show below, the model heat fluxes in the base case agree with observations to zeroth order.

Consideration of model heat fluxes also allows for a more complete evaluation of the experimental results; experiment configurations that produce reasonable seasonal variations of SST, but only at the cost of imposing unrealistic surface heat fluxes (by imposing air temperature), can be said to be inconsistent with our current understanding of the coupled system. On the other hand, forcings that can be removed, while leaving SST and heat flux behavior largely unchanged, can be said to be of, at best, secondary importance.

4. THE EXPERIMENTS

Description of the experiments

[Table 1 about here.]

The results from five numerical experiments are reported here (the wind stress field characteristics of each experiment are summarized in Table 2.) The first experiment (denoted $\mathbf{T}^X\mathbf{T}^Y$ for τ^x, τ^y,) is the baseline experiment. Both components of the seasonally averaged surface wind stress are imposed, and seasonally averaged air temperature and net solar radiation are specified in the surface heat flux boundary condition. Fig. 1 shows the zonal (τ^x) and meridional (τ^y) components of the wind stress fields used to force the model. Figs.1a, 1b show the seasonal cycle of the forcing on the equator; the forcing fields between 10°N and 10°S for March (Figs. 1c,1d) and for September (Figs. 1e, 1f) are also shown. The summer intensification of the northward meridional stress, particularly eastward of 170°W,is evident on Figs. 1b and 1 f.

[Figure 1 about here.]

The results of this baseline experiment have been compared with climatological surface data (SST and surface ship drift) and with equatorial zonal currents at 140°W and 110°W (Harrison et. al., 2000); some discrepancies with observations remain, but substantial agreement exists in the annual mean and the seasonal cycle of SST and zonal

flow and in the amplitude of the equatorial instability waves.

The remaining experiments indicated in Table 2 begin from the end of the $\mathbf{T}^X\mathbf{T}^Y$ experiment, so that at their initiation the model climatological seasonal cycle is fully developed. The second experiment is identical to $\mathbf{T}^X\mathbf{T}^Y$ except the meridional wind stress component τ^y is set equal to zero; τ^x is left unchanged and wind speed (needed for latent and sensible heat fluxes) is determined from applied τ and bulk formula (described in Model section above.) This experiment will be called $\mathbf{T}^X$.

The third experiment is identical to $\mathbf{T}^X\mathbf{T}^Y$ except that the zonal wind stress field τ^x is set equal to its annual mean value ($< \tau^x >$, where the brackets denote an annual mean quantity); this experiment will be called $<\mathbf{T}^X>\mathbf{T}^Y$. The intent of experiment $<\mathbf{T}^X>\mathbf{T}^Y$ is to explore how much of the seasonal cycle can be reproduced by the meridional wind stress when the large scale zonal structure of the circulation is maintained by the annual mean zonal wind stress field. If τ^x is set equal to zero instead of its annual average, the adjustment involves a large scale collapse of the pacific zonal temperature gradient (a 'super' el Niño), which masks the seasonal cycle; this experiment is not shown here.

The fourth experiment uses the annual mean zonal and meridional wind stress fields ($< \tau^x >$,$< \tau^y >$,) denoted as $<\mathbf{T}^X><\mathbf{T}^Y>$. The intent of $<\mathbf{T}^X><\mathbf{T}^Y>$ is to examine how much of the seasonal cycle can be reproduced by the imposed seasonally varying atmospheric forcing (e.g., air temperature; solar radiation) with annual mean

zonal and meridional wind stress.

The final (fifth) experiment, denoted as $\mathbf{T}^X\mathbf{T}^Y < Q >$, uses the full time-varying wind stress field, but instead of computing the surface heat flux each time step, imposes a constant surface heat flux. The constant heat flux used in $\mathbf{T}^X\mathbf{T}^Y < Q >$ is the annual mean (but spatially varying) heat flux computed in experiment $\mathbf{T}^X\mathbf{T}^Y$. The intent of$\mathbf{T}^X\mathbf{T}^Y < Q >$ is to examine how much of the seasonal cycle in the eastern Pacific can be reproduced from the dynamical effects of wind stress alone.

Results of the Experiments

[Figure 2 about here.]

First consider the seasonal cycle of SST in the various experiments (Fig. 2); instability wave variability has been largely removed by filtering with a 30 day running average. The smoothed COADS SST is also shown (Fig. 2a). Both the COADS data and all the experiments show the Boreal Springtime weakening of the zonal SST gradient, with warmest temperatures occurring in March and coldest temperatures in September/October in the eastern Pacific. The COADS data shows a minimum temperature of 21°C, several degrees colder than the experiments. There is much less seasonal variability in the central and western Pacific, and the data and $\mathbf{T}^X\mathbf{T}^Y$ agree. The $\mathbf{T}^X$, $<\mathbf{T}^X>\mathbf{T}^Y$ and $<\mathbf{T}^X><\mathbf{T}^Y>$ experiments reproduce most of the aspects of SST variability of the $\mathbf{T}^X\mathbf{T}^Y$ experiment, but temperatures in the far-eastern Pacific (80-100°W)

are typically one degree warmer than in $\mathbf{T}^X\mathbf{T}^Y$. For $\mathbf{T}^X$, except in the far-eastern Pacific, the zonal stress alone is able to reproduce the essential features of the seasonal cycle of SST. Experiments $<\mathbf{T}^X>\mathbf{T}^Y$ and $<\mathbf{T}^X><\mathbf{T}^Y>$ are unable to sufficiently generate a SST seasonal cycle west of 140°W, where variations in zonal stress presumably drive the system. The $<\mathbf{T}^X><\mathbf{T}^Y>$ experiment, forced only through the surface heat-flux boundary condition, shows very little SST variation west of 120°W and only weak seasonal SST variation at 110°W. Wind stress alone, without a time-varying surface heat flux ($\mathbf{T}^X\mathbf{T}^Y<Q>$), produces an SST cycle with temperatures in the western Pacific that are several degrees too warm, and unrealistic SST in the far eastern Pacific. These last two cases suggest that both time varying surface heat flux and wind stress are required to reproduce the seasonal cycle of SST. Either one, acting alone, is insufficient.

[Figure 3 about here.]

[Figure 4 about here.]

Figs. 3 and 4 show the monthly-averaged fields of SST between 10°S and 10°N, for the COADS seasonal dataset and for each experiment. Monthly averages are shown for March and September. The $\mathbf{T}^X\mathbf{T}^Y$ results show the strengthening and weakening of the cold tongue, the large changes off the south American coast and the shifting of the warmest western Pacific waters from northern to southern hemisphere that are all characteristic of Tropical Pacific SST variation. The model does not warm as much in the eastern Pacific in Boreal Spring as is suggested in climatological SST COADS data, and minimum temperatures in the cold tongue are about a degree off. $\mathbf{T}^X$ again reproduces

all of the major equatorial and western Pacific aspects of $\mathbf{T}^X\mathbf{T}^Y$, but not the behavior off the south American coast. $<\mathbf{T}^X>\mathbf{T}^Y$ and $<\mathbf{T}^X><\mathbf{T}^Y>$ reproduce the seasonal cycle of SST in the eastern Pacific; in particular, they generate the cold tongue and the September upwelling along the South American coast, however the seasonal cycle of SST is not well represented in the western Pacific. For $<\mathbf{T}^X><\mathbf{T}^Y>$ the weakening of both the cold tongue and the coastal upwelling in March is underestimated. The $\mathbf{T}^X\mathbf{T}^Y < Q >$ experiment captures the amplitude of the cold tongue west of 110°W, but there is anomalously warm water in the northern hemisphere.

[Figure 5 about here.]

Now consider the surface heat flux, as computed by the model using (2) and as reported by Oberhuber (1988) and by COADS (e.g. Esbensen and Kushnir, 1981). Fig. 5 shows the seasonal cycle at the equator for the surface heat flux anomaly, from the climatological data (Figs. 5a,b) and from the experiments (Figs. 5c-f). To generate the anomaly fields, we have subtracted the annual mean at each grid point. First, note that there is general agreement between the Oberhuber and COADS heat fluxes. The $\mathbf{T}^X\mathbf{T}^Y$ and $\mathbf{T}^X$ experiments reproduce the temporal behavior of the seasonal cycle, both in the eastern and western Pacific, in particular the maximum positive departure near the South American coast during Boreal Spring. The remaining experiments ($<\mathbf{T}^X>\mathbf{T}^Y$ and $<\mathbf{T}^X><\mathbf{T}^Y>$) do not reproduce the seasonal cycle of heat flux in the western Pacific, and the location and amplitude of the seasonal cycle in the eastern Pacific. There is considerable reported uncertainty in the COADS data; the $\mathbf{T}^X\mathbf{T}^Y$ heat flux is very close to the COADS data west of 130°W, and, while underestimating the heat flux

east of 130°W, still falls within one standard deviation of the observations. The $\mathbf{T}^X\mathbf{T}^Y$ model has a net heat flux into the ocean at the equator, verifying that the model can act to transport heat meridionally and vertically as we would expect [criticism (a) above notwithstanding].

The subsurface zonal currents produced at (140°W, 0°N) by $\mathbf{T}^X\mathbf{T}^Y$ (Fig. 6) agrees well with in-situ data from the TAO array. This climatological data, shown in the last panel of Fig. 6, was made by monthly-averaging observed zonal velocity from an upward-looking acoustic Doppler profiling current meter (ADCP) mooring at (140°W, O°N) over the period 1990-1998 (Yu and McPhaden, 1999). This process smooths out the TIWs signature in the TAO data. Note that, on these figures, blue colors denote westward flow, and red colors denote eastward flow. The seasonal reversal of the normally westward surface flow in late Boreal Spring (March-June), when the TIWs subside and the climatological westward winds are weakest, and when the upper part of the Equatorial Undercurrent (EUC) reaches its maximum speed, is well simulated. The seasonal evolution above the core of the EUC is different from that below the core, also consistent with observations (see Harrison, et. al., 2000, for these comparisons.) Experiments $\mathbf{T}^X$ and $\mathbf{T}^X\mathbf{T}^Y <\mathbf{Q}>$ reproduce the seasonal cycle of zonal velocity at (140°W, 0°N), consistent with the notion that this process is coupled primarily to the seasonal cycle of zonal wind stress.

[Figure 6 about here.]

Experiments $<\mathbf{T}^X>\mathbf{T}^Y$ and $<\mathbf{T}^X><\mathbf{T}^Y>$ (forcing by surface heat flux and/or

meridional wind stress alone) are unable to reproduce the main features of the seasonal cycle of surface and subsurface currents.

This result also extends to the basin-wide seasonal cycle of equatorial surface zonal currents (Fig.7). $\mathbf{T}^X$ reproduces the basin-wide Boreal Spring and western Pacific Boreal Winter eastward surface current episodes very much as they are seen in $\mathbf{T}^X\mathbf{T}^Y$. As would be expected, $<\mathbf{T}^X><\mathbf{T}^Y>$ is unable to reproduce any of the main features of the surface flow in $\mathbf{T}^X\mathbf{T}^Y$; while $<\mathbf{T}^X>\mathbf{T}^Y$ approximates the seasonal cycle only in the extreme eastern Pacific; the mechanism for the suppression of the TIWs and the spring current reversal is absent, and TIWs persist all year. $\mathbf{T}^X\mathbf{T}^Y <\mathbf{Q}>$ generates the seasonal cycle, but the eastward velocity magnitudes are too high in the western part of the basin. Evidently, the lack of a time-varying heat flux requires more transport of heat by near-surface currents.

We may quantify the degree to which the different experiments resemble the 'baseline' experiment ($\mathbf{T}^X\mathbf{T}^Y$) by computing a 'global' or rms error ϵ over a model year in the following way (e.g. for SST):

$$\epsilon_{SST} = \frac{1}{N_k}\sum_k [\sum_j \sum_i \frac{(SST_{ijk} - SST_{ijk}^{T^X T^Y})^2}{N_i N_j}]^{1/2} \tag{7}$$

where the i and j sums are taken over the model latitude-longitude grid points, the k sum is taken over time snapshots from a model year, and where N_i, N_j; and N_k represent the number of grid points in latitude, longitude and time, respectively. Table 3 shows

the results for SST, zonal velocity and meridional velocity. For each case, grid points at latitudes from 5°S to 5°N were summed, and ϵ was computed for four different longitude regions: the entire equatorial waveguide (131°E-70°W), the western Pacific (west of the dateline: 131°E-180°W), the predominant trade wind region (95°W-180°W), and the extreme eastern Pacific (95°W-70°W). For $\mathbf{T}^X$, errors get progressively worse as you go east. For the western Pacific, $\mathbf{T}^X$ reproduces $\mathbf{T}^X\mathbf{T}^Y$ better than the other experiments, but in the extreme eastern Pacific $\mathbf{T}^X$ does worse than the experiment with annual mean zonal stress and with either time-varying ($<\mathbf{T}^X>\mathbf{T}^Y$) or annual mean ($<\mathbf{T}^X><\mathbf{T}^Y>$) meridional stress included. Experiment $\mathbf{T}^X\mathbf{T}^Y <\mathbf{Q}>$ does considerably worse for SST, but average for reproducing the currents.

[Table 2 about here.]

[Figure 7 about here.]

5. Conclusions

Although many previous numerical studies of the eastern tropical Pacific (see Table 1) have been able to essentially reproduce the seasonal cycle of SST, there is no consensus for its fundamental cause; different mechanisms have been invoked in each case, and conclusions about the relative importance of different components of the surface forcing are different. Our baseline PE model of the Pacific ($\mathbf{T}^X\mathbf{T}^Y$), also reproduces the climatological seasonal cycle of SST well. The $\mathbf{T}^X\mathbf{T}^Y$ results show the strengthening and weakening of the cold tongue, the large changes off the south American coast and the shifting of

the warmest western Pacific waters from northern to southern hemisphere that are all characteristic of Tropical Pacific SST variation. The subsurface zonal currents produced at (140°W, 0°N) by $\mathbf{T}^X\mathbf{T}^Y$ agree well with in-situ data from the TAO array. The seasonal reversal of the normally westward surface flow in late Boreal Spring (March-June), when the TIWs subside and the climatological westward winds are weakest, and when the upper part of the Equatorial Undercurrent (EUC) reaches its maximum speed, is well simulated. We are not restoring our system any more strongly than others (e.g., Kessler or Seager). Our seasonal cycle experiment ($\mathbf{T}^X\mathbf{T}^Y$) is self-consistent in the sense defined in Section 2 above: forced by the climatological winds, air temperature and solar radiation, the computed surface heat flux, SST, currents and vertical density structure are consistent with climatological observations.

Because the surface heat flux boundary condition is critical in this context, in Section 3 we have discussed the role of our surface heat flux boundary condition in the near-surface heat equation. In particular, we have shown that Seager's criticism of the "Haney-type" boundary condition (Haney, 1971) does not apply. SST emerges as an independent quantity in our model.

In a series of numerical experiments where we have removed elements of the atmospheric forcing, we find that the different cases all produce relatively realistic seasonal cycles of SST. Although the SST signal is quite robust, only the most complete model is also able to reproduce the seasonal cycle of near surface currents and tropical instability waves (TIWs), with consistent heat fluxes.

The $<\mathbf{T}^X>\mathbf{T}^Y$ and $<\mathbf{T}^X><\mathbf{T}^Y>$ experiments reproduce most aspects of SST variability seen in the $\mathbf{T}^X\mathbf{T}^Y$ experiment, but they do so only with the imposition of surface heat fluxes that are largely inconsistent with the observation-based estimates of surface heat fluxes considered here (including in the eastern Pacific.) On the other hand, we have found that a model simulation made with the zonal wind stress alone ($\mathbf{T}^X$) reproduces very well the equatorial seasonal behavior (e.g. in SST and surface heat fluxes) of the climatological experiment ($\mathbf{T}^X\mathbf{T}^Y$,) except in the far eastern Pacific (east of 100°W). Thus, the effects of meridional stress are not negligible, but neither are they crucial. In this sense, the experiments confirm some results reported by Kessler et al. (1998,) on the relative influence of meridional winds. Additionally, the simultaneous consideration of SST and surface heat flux has shown zonal stress variations to be the more fundamental forcing function in the context of the experiments described here. For $\mathbf{T}^X$, errors get progressively worse as you go east. For the western Pacific, $\mathbf{T}^X$ reproduces $\mathbf{T}^X\mathbf{T}^Y$ better than the other experiments, but in the extreme eastern Pacific $\mathbf{T}^X$ does worse than the experiment with annual mean zonal stress and with either time-varying ($<\mathbf{T}^X>\mathbf{T}^Y$) or annual mean ($<\mathbf{T}^X><\mathbf{T}^Y>$) meridional stress included.

Wind stress alone, without a time-varying surface heat flux ($\mathbf{T}^X\mathbf{T}^Y<\mathbf{Q}>$) produces an SST cycle with temperatures in the western Pacific that are several degrees too warm, and unrealistic SST in the far eastern Pacific. In this case, however, currents are still reproduced reasonably. Thus, currents are forced mainly by wind stress, while the sea-

sonal cycle of SST depends strongly on seasonal variations in surface heat flux.

A model simulation made with the annual mean winds, forced only through the surface heat-flux boundary condition ($<\mathbf{T}^X><\mathbf{T}^Y>$) generates a seasonal cycle of SST that is superficially in agreement with data; in particular, it generates the cold tongue and the September upwelling along the South American coast. However the seasonal cycle of SST is not well represented west of 120°W, and this case does not yield consistent heat fluxes or currents. In the absence of seasonally varying currents, this system is forced relatively strongly by the seasonal cycle of air temperature, and tropical instability waves are present all year long and presumably are largely responsible for the required heat transfer. These last two cases ($\mathbf{T}^X\mathbf{T}^Y <\mathbf{Q}>$ and $<\mathbf{T}^X><\mathbf{T}^Y>$) suggest that both time varying surface heat flux and wind stress are required to reproduce the seasonal cycle of SST. Either one, acting alone, is insufficient.

Including the annual mean zonal wind stress and the seasonally varying meridional wind stress ($<\mathbf{T}^X>\mathbf{T}^Y$) appears to reproduce the September $\mathbf{T}^X\mathbf{T}^Y$ cold tongue. In particular this is the only case (other than the baseline $\mathbf{T}^X\mathbf{T}^Y$) that generates cold upwelled water off the South American coast. The cold tongue, however, does not get advected westward as much as required. $<\mathbf{T}^X>\mathbf{T}^Y$ does not adequately simulate either the surface heat flux or the surface equatorial zonal flow. While the mean large scale structure of the subsurface zonal flow field is maintained by the mean zonal stress, the varying meridional stress does not drive much seasonal variation in these fields.

In a seminal study, Philander and Pacanowski (1981) showed that switching on a uniform northward wind stress (0.5 dyne/cm^2) over a resting ocean (with idealized vertical temperature profile) produced a pool of cool water in the southeastern part of the rectangular domain, and an equatorial cold tongue with a significant meridional temperature gradient just north of the equator. They further showed that forcing with meridionally uniform, time-varying (zero to 1.0 dyne/cm^2 over a period of 200 days) northward winds, in the eastern part of the basin, can also maintain a somewhat weaker cold tongue. From these results they suggested that the meridional winds alone may be responsible for much of the observed seasonal SST variability in the eastern equatorial Atlantic and Pacific ocean. Since this study, a number of authors have made similar claims for the Pacific (e.g. Mitchell and Wallace 1992) and much effort has been directed toward understanding the influence of meridional winds. In contrast to this perspective, we find that the zonal stress alone drives much of the observed SST variability in the eastern Pacific. In our model, the cold tongue is reestablished without τ^y (i.e., experiment $\mathbf{T}^X$.) These results provide guidance for current efforts to evaluate and develop realistic coupled air-sea models. Recently, de Szoerke and Xie (2008) have drawn attention to the effects that errors in τ^y have on the seasonal cycle of equatorial Pacific SST in coupled air-sea models. Results of our study suggest that, while consideration of τ^y is warranted and perhaps pertinent to the models considered by de Szoerke and Xie (2008,) realistic coupled model behavior should be at least as sensitive to variability (errors or otherwise) in τ^x as τ^y, and thus, in order to be realistic, it will be fundamentally important for such models to predict accurate zonal winds.

While the discussion about the relative importance of the surface heat flux and meridional wind stress field in the seasonal cycle of SST will undoubtedly continue, and perhaps be assisted by future coupled ocean-atmosphere experiments, the experiments reported here indicate that the upper ocean equatorial fields in this ocean circulation model are largely zonal wind stress driven. Meridional stress has little effect except in the easternmost Pacific. More importantly, we have shown that merely reproducing the seasonal cycle of SST does not allow conclusions about dynamics and forcing mechanisms to be made. This leads to the disconcerting notion that using a standard approach, i.e., using a hierarchy of models, starting with the simplest and moving toward more realism as understanding is gained, may be inappropriate.

Acknowledgments

The Thermal Modeling and Analysis Project (TMAP) at PMEL provided programming assistance and the Ferret analysis program was used in the analysis of the model outputs (http://tmap.pmel.noaa.gov/ferret). This is PMEL contribution # 2913 and JISAO publication #

Appendix: The term balances in the temperature equation

Fig. 8 shows the nonlinear terms -u∂T/∂x, -v∂T/∂y and -w∂T/∂z (based on $\mathbf{T}^X\mathbf{T}^Y$) from Eq. 6, averaged over a latitude band 2°S-2°N, over a depth range 0-30 m, and over a model year. Also shown on Fig. 8 is an estimate of the heat flux term <Q>/(ρ c_p Δz), where we have used the surface heat flux for Q, and where we have assumed Δz=30 m [6]. In the eastern Pacific, vertical advection of heat is as large an effect as the surface heat flux; zonal and meridional advection terms are also non-negligible. In the western Pacific, zonal advection is the dominant nonlinear effect.

[Figure 8 about here.]

REFERENCES

Arakawa, A. (2004) The cumulus parameterization problem: past, present and future *J. Climate*, **17**, 2493–2525.

Bonjean, F. (2001) Influence of surface currents on the sea surface temperature in the tropical Pacific Ocean. *J. Phys. Oceanogr.*, **31**, 943-961.

Borovikov, A., M.M. Rienecker and P.S. Schopf (2000) Surface heat balance in the equatorial Pacific ocean: climatology and the warming event of 1994-1995. *J. Climate*,

[6]The depth dependence of the heat flux is handled by MOM2 in a much more detailed way (see Eqs. 2–5), and this choice for 'mixed layer' depth Δz is somewhat arbitrary

14, 2624–2641.

Bryan, K. (1969) A numerical method for the study of the circulation of the World Ocean. *J. Comput. Phys.*, **4**, 347–376.

Cane, M. A. (1979) Response of an Equatorial Ocean to Simple Wind Stress Patterns, 1: Model Formulation and Analytic Results. *J. Mar. Res.*, **37**(2), 233–252.

Cai, W., M.A. Collier and H.B. Gordon (2003) Strong ENSO variability and a super-ENSO pair in the CSIRO Mark 3 Coupled Climate Model. *Mon. Wea. Rev.*, **131**, 1189–1210.

Chen, D., L. M. Rothstein, and A. J. Busalacchi (1994a) A hybrid vertical mixing scheme and its application to tropical ocean models. *J. Phys. Oceanogr.*, **24**, 7725–7741.

–, A. J. Busalacchi, and L. M. Rothstein (1994b) The roles of vertical mixing, solar radiation and wind stress in a model simulation of the sea surface temperature seasonal cycle in the tropical Pacific Ocean. *J. Geophys. Res.*, **99**, 20345–20359.

Chang, P. (1994) A study of the seasonal cycle of sea surface temperature in the tropical Pacific Ocean using reduced gravity models. *J. Geophys. Res.*, **99**, 7725-7741.

Chang, P. and S.G.H. Philander (1994) A coupled ocean-atmopshere instability of relevance to the seasonal cycle. *J. Atmos. Sci.*, **51**, 3627-3648.

Chang, P. (1996) The role of the dynamic ocean-atmopshere interactions in the tropical seasonal cycle. *J. Climate*, **9**, 2973-2985.

Cox, M.D. (1984) A Primitive Equation, 3-Dimensional Model of the Ocean. GFDL Ocean Group Technical Report No. 1. 143pp.

Cronin, M. F., N.A. Bond, C.W. Fairall and R.A. Weller (2006) Surface cloud forcing in the east Pacific stratus deck/cold tongue/ITCZ complex. *J. Climate*, **19**, 392–409.

Davey M. K., M. Huddleston, K. R. Sperber and the Model Data Contributors (2002) STOIC: A study of coupled model climatology and variability in tropical ocean regions. *Climate Dyn.*, **18**, 403–420.

de Szoeke, S.P. and S.-P. Xie (2008) The tropical eastern Pacific seasonal cycle: assessment of errors and machanisms in IPCC AR4 coupled-atmosphere general circulation models. *Journal of Climate*, **21**, 2573–2590.

Delecluse, P., M.K. Davey, Y. Kitamura, S.G.H. Philander, M. Suarez and L. Bengtsson. (1998) Coupled general circulation modeling of the tropical Pacific. *J. Geophys. Res.*, **103**, 14357–14373.

DeWitt, D.G. and E.K. Schnieder (1999) The processes determining the annual cycle of equatorial sea surface temperature: A coupled general circulation model perspective. *Mon. Wea. Rev.*, **127**, 381–395.

Enfield, D. B. (1986) Zonal and seasonal variations of the near-surface heat balance of the equatorial Pacific Ocean. *J. Phys. Oceanogr.*, **16**, 1038–1054.

Esbensen, S. K. and Y. Kushnir (1981) The heat budget of the global ocean: An atlas based on estimates from surface marine observations., Climatic Research Institute Report No 29, Oregon State University.

Fu, X. and B. Wang (2001) A coupled modeling study of the seasonal cycle of the Pacific Cold Tongue part I: Simulation and sensitivity experiments. *J. Climate*, **14**, 765–779.

Gent, P. R. and M. A. Cane (1989) A Reduced Gravity, Primitive Equation Model of the Upper Equatorial Ocean. *J. Comput. Phys.*, **81**(2), 444–480.

Giese, B. and J. Carton (1994) The seasonal cycle in a coupled ocean-atmosphere model. *J. Climate*, **7**, 1208–1217.

Gordon, C. and R.A. Corry (1991) A model simulation of the seasonal cycle in the tropical Pacific Ocean. *J. Geophys. Res*, **96**, 847–864.

Guilyardi E. (2000) El Niño-mean state-seasonal cycle interactions in a multi-model ensemble. *Clim. Dyn.* **26**, 329–348.

Haney, R.L., (1971) Surface thermal boundary conditions for ocean circulation models. *J. Phys. Oceanogr.*, **1**, 241–248.

Harrison, D.E. (1989) On climatological monthly mean wind stress and wind stress curl fields over the world ocean. *J. Climate*, **2**(1), 57–70.

Harrison, D.E., W.S. Kessler, and B.S. Giese (1989) Ocean circulation model hindcasts of the 1982-83 El Niño: Thermal variability along the ship-of-opportunity tracks. *J. Phys. Oceanogr.*, **19**(4), 397–418.

Harrison, D.E., B.S. Giese, and E.S. Sarachik (1990) Mechanisms of SST change in the equatorial waveguide during the 1982-83 ENSO. *J. Climate*, **3**, 173–188.

Harrison, D.E., G.A. Vecchi, and R.H. Weisberg (2000) Eastward surface jets in the central equatorial Pacific, November 1992-March 1992. *J. Mar. Res.*, **58**(5), 735–754.

Harrison, D.E., R.D. Romea, and S.H. Hankin (2001) Central equatorial Pacific zonal currents. I: The Sverdrup balance, nonlinearity and tropical instability waves. Annual mean dynamics. *J. Mar. Res.*, **59**(6), 895–919.

Harrison, D.E., R.D. Romea, and G.A. Vecchi (2001) Central equatorial Pacific zonal currents. II: The seasonal cycle and the boreal spring surface eastward surge. *J. Mar. Res.*, **59**(6), 921–948.

Harrison, D.E., and A.M. Chiodi (2008) Pre and post 1997/1998 westerly wind events and equatorial Pacific cold tongue warming. *J. Climate.* [to appear]

Hayes, S. P., P. Chang, and M. J. McPhaden (1991) Variability of the sea surface temperature in the eastern equatorial Pacific during 1986-1988. *J. Geophys. Res.*, **96**, 10553–10566.

Horel, J.D. (1982) On the annual cycle of the tropical Pacific atmosphere and ocean. *Mon. Wea. Rev.*, **110**, 1863-1878.

Kessler, W.S., L.M. Rothstein and D. Chen (1998) The annual cycle of SST in the eastern tropical Pacific, diagnosed in an ocean GCM. *J. Climate*, **11**, 777–799.

Killworth, P.D., D.A. Smeed and A.J.G. Nurser (2000) The effects on ocean models of relaxation toward observations at the surface. *J. Phys. Oceanogr.*, **30**, 160–174.

Kraus, E. B., and J. S. Turner, 1967: A one-dimensional model of the seasonal thermocline. II: The general theory and its consequences. *Tellus*, 19, 98?105.

Köberle, C. and S.G.H. Philander (1994) On the processes that control seasonal variations of sea surface temperatures in the tropical Pacific ocean. *Tellus*, **46**A, 481–496.

Latif, M., (1987) Tropical Ocean Circulation Experiments. *J. Phys. Oceanogr.*, **17**, 246–263.

Latif, M. and co-authors (2001): ENSIP: The El Niño Simulation Intercomparison Project. *Climate Dynamics*, **18**, 255–276.

Large, W., and S. Pond (1981) Open Ocean Momentum Flux Measurements in Moderate to Strong Winds. *J. Phys. Oceanogr.*, **11**, 324–336.

Levitus, S. (1982) Climatological Atlas of the World Ocean. NOAA Professional Paper 13, U.S. Government Printing Office, Washington, DC, 173 pp.

Levitus, S. (1987) A comparison of the annual cycle of two sea surface temperature climatologies of the world ocean. *J. Phys. Oceanogr.*, **17**, 197–214.

Li, T. and S.G.H. Philander (1996) On the annual cycle of the eastern equatorial Pacific. *J. Climate*, **9**, 2986–2998.

Lindzen, R.S. and S. Nigam (1987) On the role of sea-surface temperature gradients in forcing low-level winds and convergence in the Tropics. *J. Atmos. Sci.*, **44**, 2418–2436.

Mechoso, C. S., and Coauthors, 1995: The seasonal cycle over the tropical Pacific in coupled ocean-atmosphere General Circulation Models. *Mon. Wea. Rev.*, **123**, 2825–2838.

Mitchell, T. P., and J. M. Wallace, 1992: On the annual cycle in equatorial convection and sea surface temperature. *J. Climate*, **5**, 1140–1156.

Neelin, J.D. (1991) The slow sea surface temperature mode and the fast-wave limit: Analytic theory for tropical interannual oscillations and experiments in a hybrid coupled model. *J. Atmos. Sci.*, **48**, 584–606.

Nigam, S. and Y. Chao (1996) Evolution dynamics of tropical ocean-atmosphere annual cycle variability. *J. Climate*, **9**, 3187–3205.

Oberhuber, J. M. (1988) An atlas based on the COADS dataset: The budgets of heat, buoyancy, and turbulent kinetic energy at the surface of the global ocean. Max-Planck-Institut für Meteorologie Rep. No. 15, 20 pp 1 plates.

Pacanowski, R. C., and S. G. H. Philander, (1981) Parameterization of vertical mixing in numerical models of tropical oceans. *J. Phys. Oceanogr.*, **11**(11), 1443–1451.

Perigaud, C., F. Melin, and C. Cassou (2000) ENSO simulated by intermediate coupled models and evaluated with observations over 1970-98. Part I: Role of the Off-Equatorial Variability. *J. Climate*, **13**, 1605–1634.

Philander, S. G. H., and R. C. Pacanowski (1981) The oceanic response to cross-equatorial winds (with application to coastal upwelling in low latitudes). *Tellus*, **33**, 201–210.

Philander, S.G.H. and A.D. Siegel, (1985) Simulation of El Niño of 1982-1983, *Coupled Ocean-Atmosphere Models* J. Nihoul, Ed., Elsevier, 517–541.

Philander, S. G. H., W. J. Hurlin, and A. D. Siegel, (1987) Simulation of the seasonal cycle of the tropical Pacific Ocean. *J. Phys. Oceanogr.*, **17**(11), 1986–2002.

Price, J. F., R. A. Weller, and R. Pinkel (1986) Diurnal cycling: Observations and models of the upper ocean response to diurnal heating cooling and wind mixing. *J. Geophys. Res.*, **91**, 8411–8427.

Robertson, A. W., C.-C. Ma, C. R. Mechoso, and M. Ghil, 1995: Simulation of the tropical Pacific climate with a coupled ocean atmosphere general circulation model. Part I: The seasonal cycle. *J. Climate*, **8**, 1178–1198.

Schneider, E.K. (2002) Understanding differences between the equatorial Pacific as simulated by two coupled GCMs. *J. Climate*, **15**, 449–469.

Seager, R., S. E. Zebiak, and M. A. Cane, (1988) A model of the tropical Pacific sea surface temperature climatology. *J. Geophys. Res.*, **93**, 1265–1280.

Seager, R. (1989) Modeling tropical Pacific sea surface temperature: 1970-98. *J. Phys. Oceanogr.*, **19**, 419–434.

Seager, R. and B. Blumenthal (1994) Modeling tropical Pacific sea surface temperature with satellite-derived solar radiative forcing. *J. Climate*, **7**, 1943-1957.

Seager, R., Y. Kushnir, and M. A. Cane (1995) On heat flux boundary conditions for ocean models. *J. Phys. Oceanogr.*, **25**, 3219–3230.

Seager, R, M.B. Blumenthal and Y. Kushnir, (1995) An advective atmospheric mixed layer model for ocean modeling purposes: global simulation of surface heat fluxes. *J. Climate*, **8**, 1951–1964.

Semtner, A.J. (1974) An Oceanic General Circulation Model with Bottom Topography. UCLA Dept. of Meteorology Tech. Rep. No. 9, 99pp.

Schopf, P. S., and A. Loughe (1995) A reduced-gravity isopycnal ocean model: Hindcasts of El Niño. *Mon. Wea. Rev.*, **3**, 2839–2863.

Swenson, M.S. and D.V. Hansen (1999) Tropical Pacific ocean mixed layer heat budget: The Pacific cold tongue. *J. Phys. Oceanogr.*, **29**, 69–81.

Takeuchi, K., (1986) Numerical study of the seasonal variations of the subtropical front and the subtropical countercurrent. *J. Phys. Oceanogr.*,**16**, 919–926.

Tozuka, T. and T. Yamagata (2003) Annual ENSO. *J. Phys. Oceanogr.*, **33**, 1564–1578.

Woodruff, S.D., R.J. Slutz, R.L. Jenne, and P.M. Steurer (1987) A comprehensive ocean-atmosphere data set. *Bull. Amer. Meteor. Soc.*, **68**, 1239–1250.

Wang, B. (1994) On the annual cycle in the tropical eastern central Pacific. *J. Climate*, **7**, 1926–1942.

Wang, B. and Fu, X. (2001) Processes determining the rapid reestablishment of the equatorial Pacific cold tongue/ITCZ complex. *J. Climate*, **14**, 2250–2265.

Wang, W., and M.J. McPhaden (1999) The surface layer heat balance in the equatorial Pacific Ocean, Part I: Mean seasonal cycle. *J. Phys. Oceanogr.*, **29**, 1812–1831.

Wittenberg, A.T., A. Rosati, N.-C. Lau and J.J. Ploshay (2006) GFDL's CM2 global coupled climate models. Part III: Tropical Pacific climate and ENSO. *J. Climate*, **19**, 698–722.

Wyrtki, K. (1981) An estimate of equatorial upwelling in the Pacific. *J. Phys. Oceanogr.*, **11**, 1205–1214.

Xie, S.-P. (1994) On the genesis of the equatorial annual cycle. *J. Climate*, **7**, 2008-2013.

Yu, X., and M.J. McPhaden (1999) Seasonal variability in the equatorial Pacific. *J. Phys. Oceanogr.*, **29**, 925–947.

Zebiak, S. E. and M. A. Cane (1987) A Model El-Niño Southern Oscillation. *Mon. Wea. Rev.*, **115**(10), 2262–2278.

List of Figures

1 a) Seasonal cycle of τ^x applied to the model (following Harrison 1989b) along the equator. b) Same as (a)for τ^y. c) March monthly mean τ_x. d) March monthly mean τ^y. e) September monthly mean τ_x. f) September monthly mean τ^y. 50

2 a) Seasonal cycle of COADS equatorial SST and the seasonal cycle of SST from, b) the baseline experiment ($\mathbf{T}^X\mathbf{T}^Y$), c) experiment $\mathbf{T}^X$, d) experiment $<\mathbf{T}^X>\mathbf{T}^Y$, e) experiment $<\mathbf{T}^X><\mathbf{T}^Y>$ and f) experiment $\mathbf{T}^X\mathbf{T}^Y<Q>$. 51

3 March monthly mean SST from a) COADS, c)$\mathbf{T}^X\mathbf{T}^Y$ and e) $\mathbf{T}^X$. September monthly mean SST from b) COADS, d)$\mathbf{T}^X\mathbf{T}^Y$ and f) $\mathbf{T}^X$. 52

4 March monthly mean SST from g) $<\mathbf{T}^X>\mathbf{T}^Y$, i)$<\mathbf{T}^X><\mathbf{T}^Y>$ and k) $\mathbf{T}^X\mathbf{T}^Y$ $<\mathbf{Q}>$. September monthly mean SST from h) $<\mathbf{T}^X>\mathbf{T}^Y$, j)$<\mathbf{T}^X><\mathbf{T}^Y>$ and l) $\mathbf{T}^X\mathbf{T}^Y$ $<\mathbf{Q}>$. 53

5 The seasonal cycle of equatorial heat flux from a) COADS (Esbensen and Kushnir, 1981), b) Oberhuber (1988), c) $\mathbf{T}^X\mathbf{T}^Y$, d)$\mathbf{T}^X$ and e) $<\mathbf{T}^X>\mathbf{T}^Y$ and f) $<\mathbf{T}^X><\mathbf{T}^Y>$ 54

6 The seasonal cycle of zonal velocity at 140°W, 0°N from a)$\mathbf{T}^X\mathbf{T}^Y$, b) $\mathbf{T}^X$ c) $<\mathbf{T}^X>\mathbf{T}^Y$, d)$<\mathbf{T}^X><\mathbf{T}^Y>$, e) $\mathbf{T}^X\mathbf{T}^Y$ $<\mathbf{Q}>$ and f) TAO data. . . . 55

7 The seasonal cycle of zonal velocity along the equator from a)$\mathbf{T}^X\mathbf{T}^Y$, b) $\mathbf{T}^X$ c) $<\mathbf{T}^X>\mathbf{T}^Y$, d)$<\mathbf{T}^X><\mathbf{T}^Y>$ and e) $\mathbf{T}^X\mathbf{T}^Y$ $<\mathbf{Q}>$. 56

8 Annual means of the nonlinear advection terms, -u∂T/∂x, -v∂T/∂y, -w∂T/∂z and <Q>/(c_p ρ Δz) 57

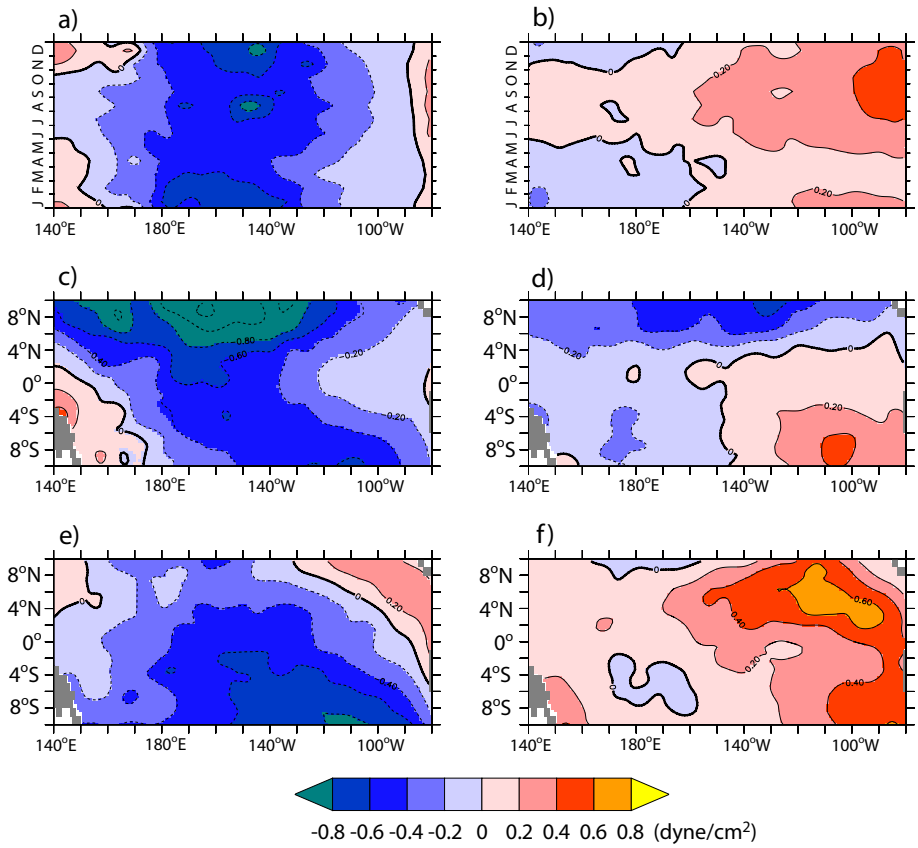

Figure 1: a) Seasonal cycle of τ^x applied to the model (following Harrison 1989b) along the equator. b) Same as (a)for τ^y. c) March monthly mean τ_x. d) March monthly mean τ^y. e) September monthly mean τ_x. f) September monthly mean τ^y.

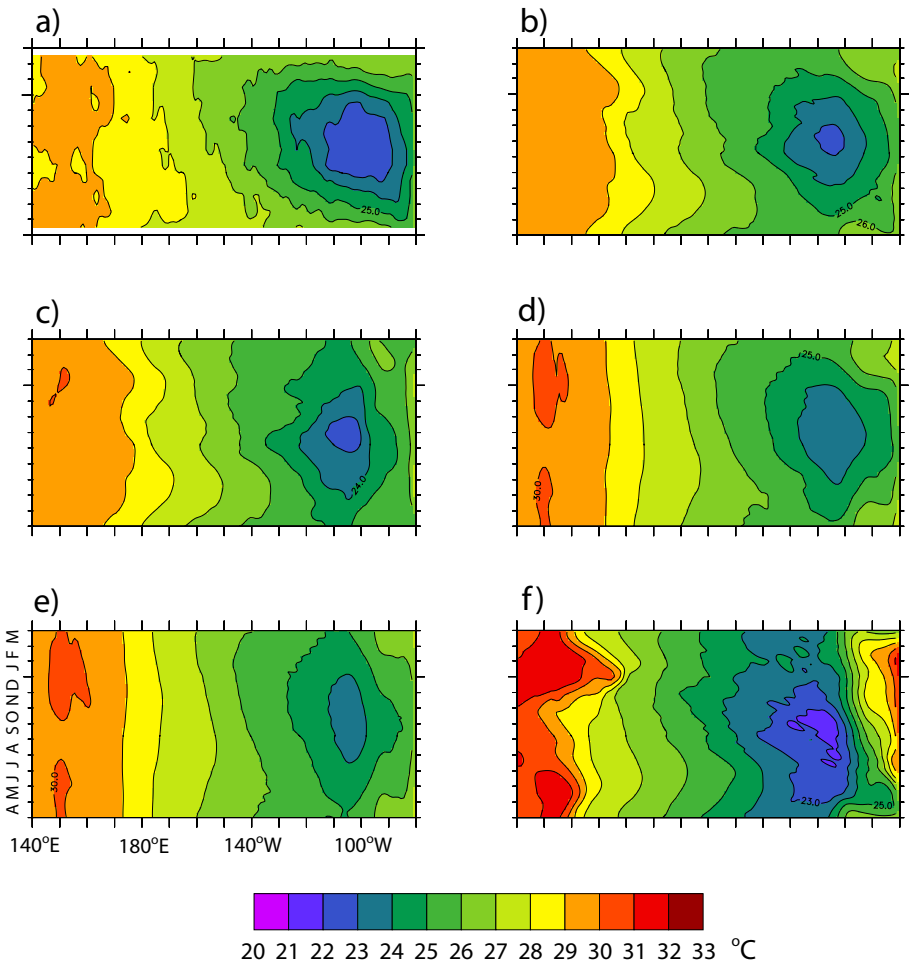

Figure 2: a) Seasonal cycle of COADS equatorial SST and the seasonal cycle of SST from, b) the baseline experiment ($\mathbf{T}^X\mathbf{T}^Y$), c) experiment $\mathbf{T}^X$, d) experiment $<\mathbf{T}^X>\mathbf{T}^Y$, e) experiment $<\mathbf{T}^X><\mathbf{T}^Y>$ and f) experiment $\mathbf{T}^X\mathbf{T}^Y<Q>$.

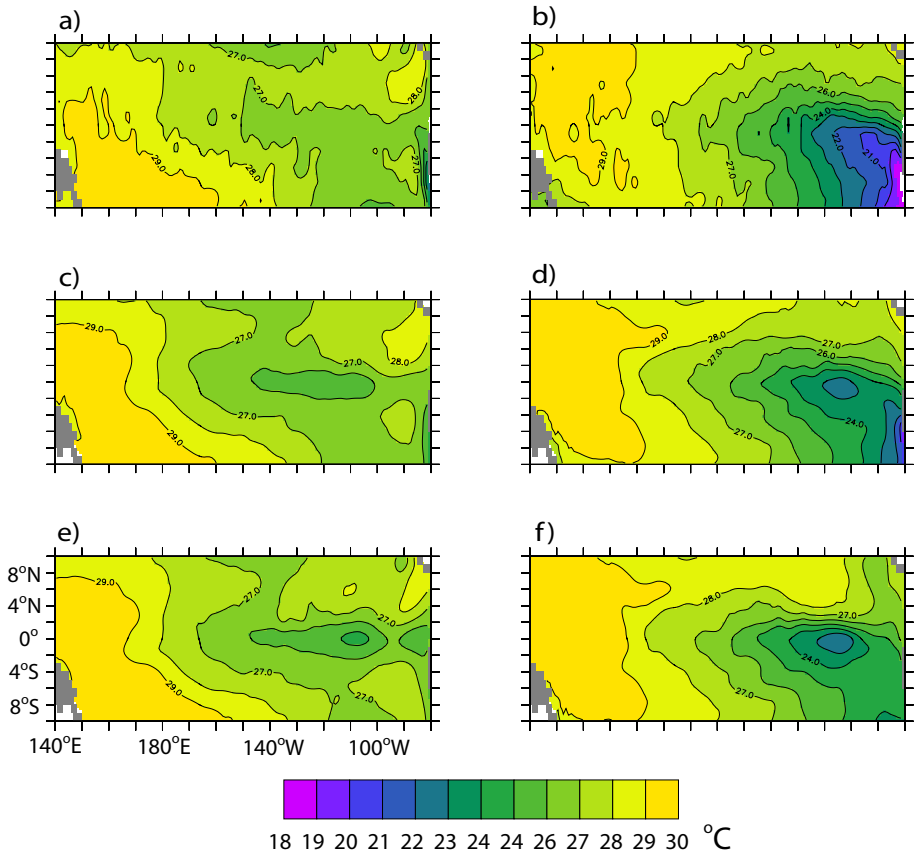

Figure 3: March monthly mean SST from a) COADS, c)$\mathbf{T}^X\mathbf{T}^Y$ and e) $\mathbf{T}^X$. September monthly mean SST from b) COADS, d)$\mathbf{T}^X\mathbf{T}^Y$ and f) $\mathbf{T}^X$.

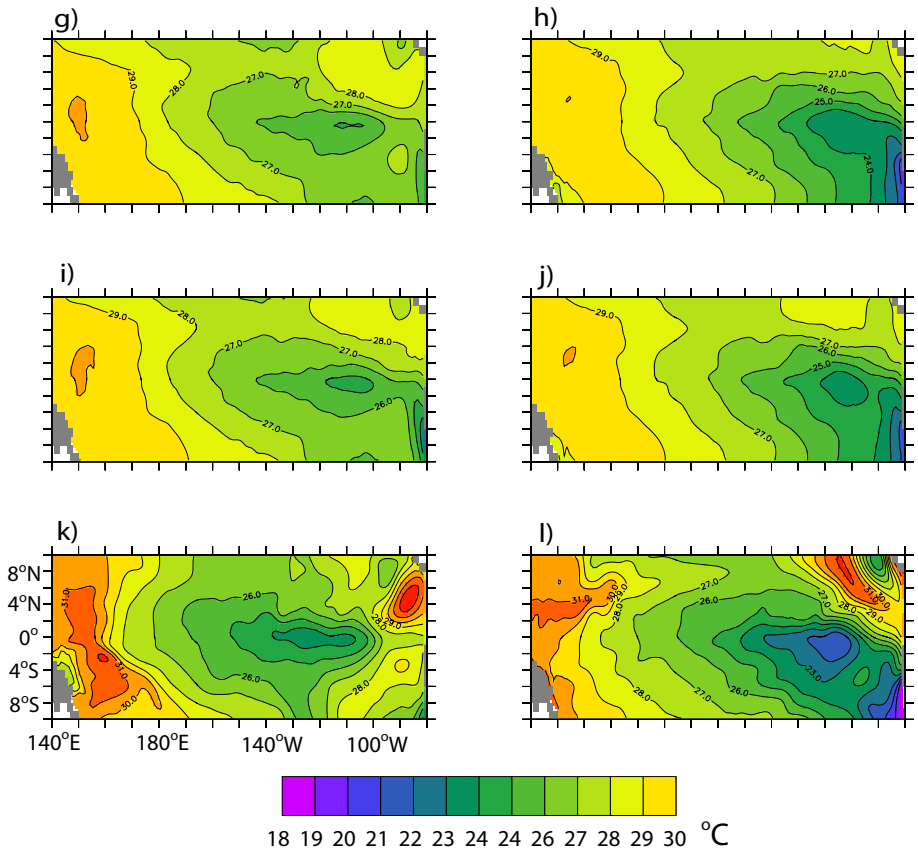

Figure 4: March monthly mean SST from g) $<\mathbf{T}^X>\mathbf{T}^Y$, i)$<\mathbf{T}^X><\mathbf{T}^Y>$ and k) $\mathbf{T}^X\mathbf{T}^Y <\mathbf{Q}>$. September monthly mean SST from h) $<\mathbf{T}^X>\mathbf{T}^Y$, j)$<\mathbf{T}^X><\mathbf{T}^Y>$ and l) $\mathbf{T}^X\mathbf{T}^Y <\mathbf{Q}>$.

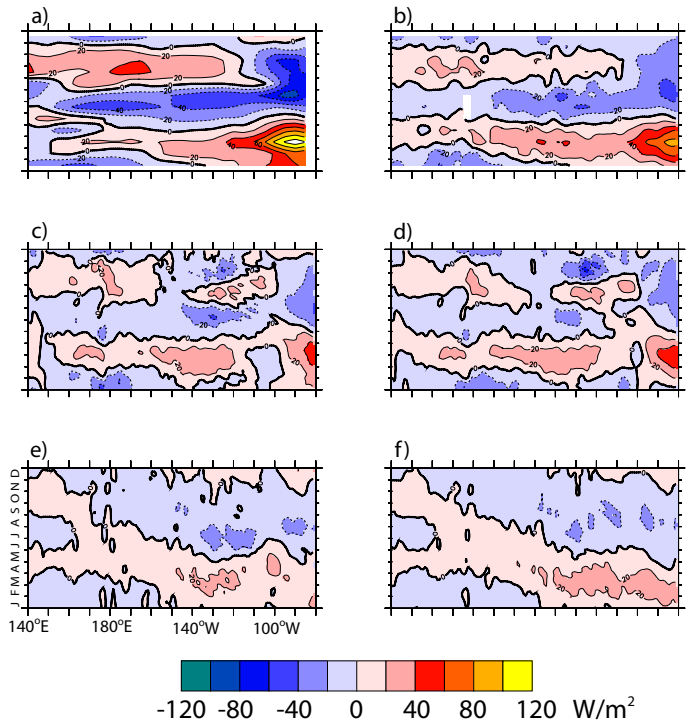

Figure 5: The seasonal cycle of equatorial heat flux from a) COADS (Esbensen and Kushnir, 1981), b) Oberhuber (1988), c) $\mathbf{T}^X\mathbf{T}^Y$, d)$\mathbf{T}^X$ and e) $<\mathbf{T}^X>\mathbf{T}^Y$ and f) $<\mathbf{T}^X><\mathbf{T}^Y>$

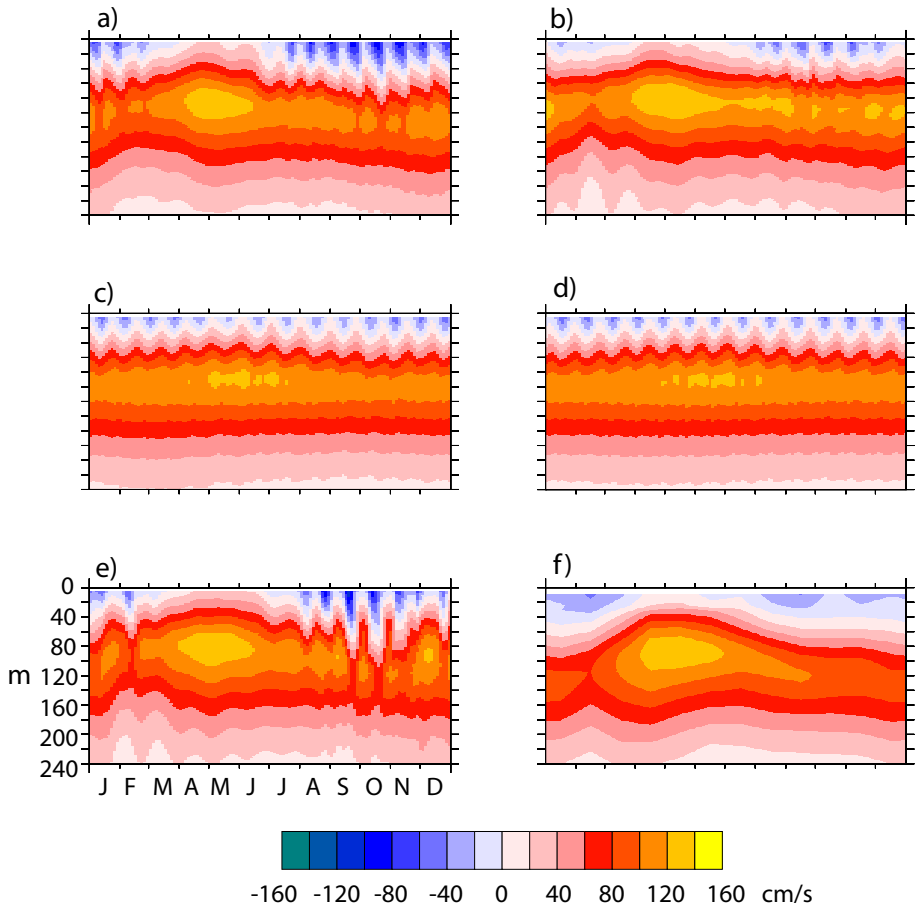

Figure 6: The seasonal cycle of zonal velocity at 140°W, 0°N from a)$\mathbf{T}^X\mathbf{T}^Y$, b) $\mathbf{T}^X$ c) $<\mathbf{T}^X>\mathbf{T}^Y$, d)$<\mathbf{T}^X><\mathbf{T}^Y>$, e) $\mathbf{T}^X\mathbf{T}^Y$ $<\mathbf{Q}>$ and f) TAO data.

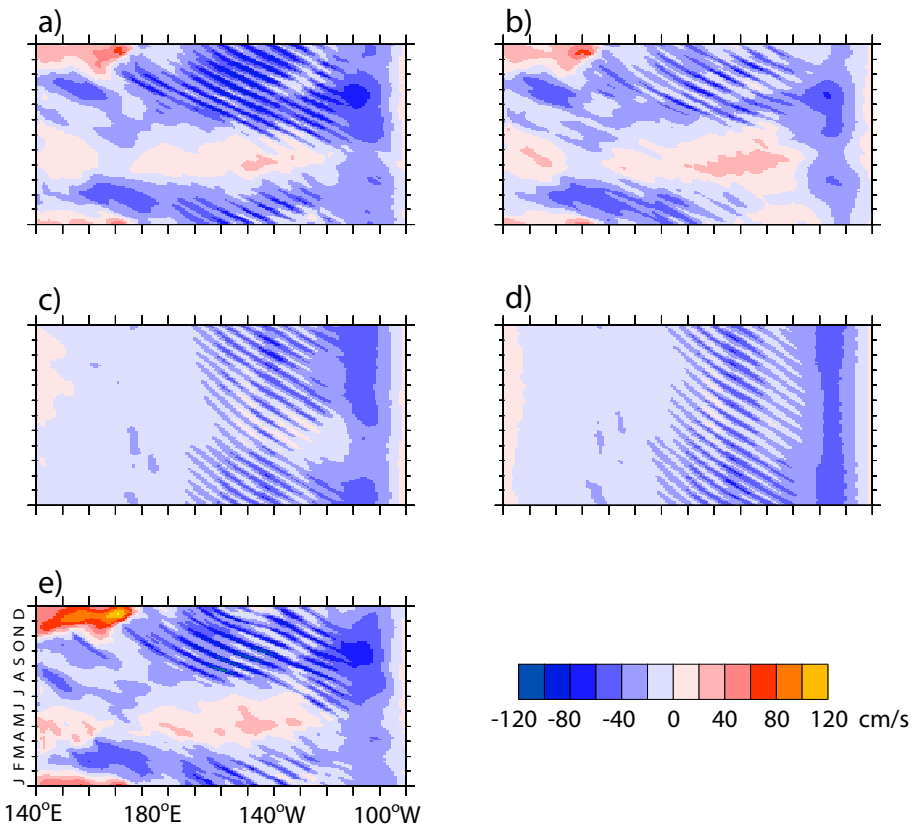

Figure 7: The seasonal cycle of zonal velocity along the equator from a)$\mathbf{T}^X\mathbf{T}^Y$, b) $\mathbf{T}^X$ c) $<\mathbf{T}^X>\mathbf{T}^Y$, d)$<\mathbf{T}^X><\mathbf{T}^Y>$ and e) $\mathbf{T}^X\mathbf{T}^Y$ $<\mathbf{Q}>$.

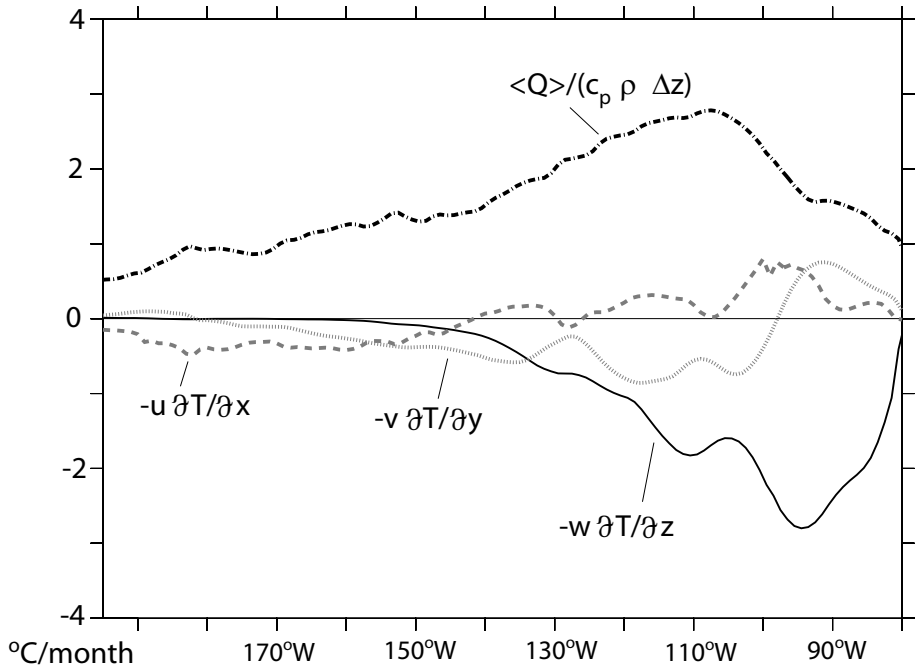

Figure 8: Annual means of the nonlinear advection terms, -u∂T/∂x, -v∂T/∂y, -w∂T/∂z and <Q>/(c_p ρ Δz)

List of Tables

1 Model Study Summary 14

2 Summary of the wind stress forcing for the numerical experiments. τ^x and τ^y are zonal and meridional wind stress, respectively. The brackets ¡¿ denote an annual mean quantity. T_{air}, and I denote that seasonal air temperature and net solar radiation are specified in the surface heat flux boundary condition, respectively; $< Q >$ denotes that annual mean surface heat flux (computed in experiment $\mathbf{T}^X\mathbf{T}^Y$) is imposed as a constant surface heat flux boundary condition. 59

3 Summary of the average (rms) error ϵ for (a) SST (°C), (b) surface zonal current u (cm/s), and (c) surface meridional currents v (cm/s). The errors were computed with Eq. 7, and represent average deviations from the baseline $\mathbf{T}^X\mathbf{T}^Y$ model run for experiments $\mathbf{T}^X$, $<\mathbf{T}^X>\mathbf{T}^Y$, $<\mathbf{T}^X>\mathbf{T}^Y$ and $\mathbf{T}^X\mathbf{T}^Y<\mathbf{Q}>$ (A summary of these experiments is listed in Table 2.) For each case, an entire seasonal cycle (model year) was used, grid points at latitudes from 5°S to 5°N were summed, and ϵ was computed for four different longitude regions: (1) the entire equatorial waveguide (131°E-70°W), (2) the western Pacific (west of the dateline: 131°E-180°W), (3) the predominant trade wind region (180°W-95°W), and (4) the extreme eastern Pacific (95°W-70°W). 60

Table 2: Summary of the wind stress forcing for the numerical experiments. τ^x and τ^y are zonal and meridional wind stress, respectively. The brackets ¡¿ denote an annual mean quantity. T_{air}, and I denote that seasonal air temperature and net solar radiation are specified in the surface heat flux boundary condition, respectively; $< Q >$ denotes that annual mean surface heat flux (computed in experiment $\mathbf{T}^X\mathbf{T}^Y$) is imposed as a constant surface heat flux boundary condition.

Experiment	Wind Stress Components				Heat Flux	
	τ^x	$< \tau^x >$	τ^y	$< \tau^y >$	T_{air},I Specified	$< Q >$ Specified
$\mathbf{T}^X\mathbf{T}^Y$	**x**		**x**		**x**	
$\mathbf{T}^X$	**x**				**x**	
$<\mathbf{T}^X>\mathbf{T}^Y$		**x**	**x**		**x**	
$\mathbf{T}^X\mathbf{T}^Y<\mathbf{Q}>$	**x**		**x**			**x**

Table 3: Summary of the average (rms) error ϵ for (a) SST (°C), (b) surface zonal current u (cm/s), and (c) surface meridional currents v (cm/s). The errors were computed with Eq. 7, and represent average deviations from the baseline $\mathbf{T}^X\mathbf{T}^Y$ model run for experiments $\mathbf{T}^X$, $<\mathbf{T}^X>\mathbf{T}^Y$, $<\mathbf{T}^X>\mathbf{T}^Y$ and $\mathbf{T}^X\mathbf{T}^Y<\mathbf{Q}>$ (A summary of these experiments is listed in Table 2.) For each case, an entire seasonal cycle (model year) was used, grid points at latitudes from 5°S to 5°N were summed, and ϵ was computed for four different longitude regions: (1) the entire equatorial waveguide (131°E-70°W), (2) the western Pacific (west of the dateline: 131°E-180°W), (3) the predominant trade wind region (180°W-95°W), and (4) the extreme eastern Pacific (95°W-70°W).

(a) ϵ_{SST}

	131°E-70°W	131°E-180°W	180°W-95°W	95°W-70°W
$\mathbf{T}^X$	0.45	0.12	0.47	0.78
$<\mathbf{T}^X>\mathbf{T}^Y$	0.33	0.23	0.38	0.29
$<\mathbf{T}^X><\mathbf{T}^Y>$	0.40	0.27	0.42	0.49
$\mathbf{T}^X\mathbf{T}^Y<\mathbf{Q}>$	1.5	1.2	1.4	2.6

(b) ϵ_u

	131°E-70°W	131°E-180°W	180°W-95°W	95°W-70°W
$\mathbf{T}^X$	15	10	17	10
$<\mathbf{T}^X>\mathbf{T}^Y$	18	17	19	7.1
$<\mathbf{T}^X><\mathbf{T}^Y>$	19	19	19	3.4
$\mathbf{T}^X\mathbf{T}^Y<\mathbf{Q}>$	15	14	16	7.0

(b) ϵ_v

	131°E-70°W	131°E-180°W	180°W-95°W	95°W-70°W
$\mathbf{T}^X$	15	8.4	18	11
$<\mathbf{T}^X>\mathbf{T}^Y$	16	8.8	19	4.8
$<\mathbf{T}^X><\mathbf{T}^Y>$	16	10	19	4.9
$\mathbf{T}^X\mathbf{T}^Y<\mathbf{Q}>$	17	10	20	6.8